

## Article

# Exploration of In Vitro Voltage Production by a Consortium of Chemolithotrophic Microorganisms Using Galena (PbS) as a Sulphur Source

Susana Citlaly Gaucin Gutiérrez<sup>1</sup>, Juan Antonio Rojas-Contreras<sup>1</sup> , David Enrique Zazueta-Álvarez<sup>2</sup> ,  
Efren Delgado<sup>3</sup> , Perla Guadalupe Vázquez Ortega<sup>1</sup> , Hiram Medrano Roldán<sup>1</sup> and Damián Reyes Jáquez<sup>1,\*</sup> 

<sup>1</sup> Department of Chemical and Biochemical Engineering, National Technological Institute of Mexico (TecNM)—Durango Institute of Technology (ITD), Felipe Pescador 1830 Ote. Col. Nueva Vizcaya, Victoria de Durango 34080, Mexico; 07040234@itdurango.edu.mx (S.C.G.G.); jrojas@itdurango.edu.mx (J.A.R.-C.); pvazquez@itdurango.edu.mx (P.G.V.O.); hmedrano@itdurango.edu.mx (H.M.R.)

<sup>2</sup> Department of Environmental Technology Engineering, Polytechnic University of Durango, Carretera Durango-México Km 9.5., Victoria de Durango 34300, Mexico; david.zazueta@unipolidgo.edu.mx

<sup>3</sup> Food Science and Technology, Department of Family and Consumer Sciences, New Mexico State University, P.O. Box 30001, Las Cruces, NM 88003-8001, USA; edelgad@nmsu.edu

\* Correspondence: damian.reyes@itdurango.edu.mx

**Abstract:** Sulphur plays a fundamental role in the biological processes of chemolithotrophic microorganisms. Due to the redox characteristics of sulphur, microorganisms use it for metabolic processes. Such is the case of the dissimilatory processes in the anaerobic respiration of reducing microorganisms. The production of electrical energy from the metabolism of native microorganisms using sulphur as substrate from inorganic mineral sources in the form of Galena (PbS) was achieved using MR mineral medium with 15% (*w/v*) of PbS mineral concentrate. At 400 h of growth, the highest voltage produced in an experimental unit under anaerobic conditions was 644 mV. The inoculum was composed of microorganisms with spiral morphology, and at the final stages of energy production, the only microorganism identified was *Bacillus clausii*. This microorganism has not been reported in bioelectrochemical systems, but it has been reported to be present in corrosive environments and reducing anoxic environments.

**Keywords:** bioelectrochemical systems; sulphur reduction; electroactive consortia



**Citation:** Gaucin Gutiérrez, S.C.; Rojas-Contreras, J.A.; Zazueta-Álvarez, D.E.; Delgado, E.; Vázquez Ortega, P.G.; Medrano Roldán, H.; Reyes Jáquez, D. Exploration of In Vitro Voltage Production by a Consortium of Chemolithotrophic Microorganisms Using Galena (PbS) as a Sulphur Source. *Clean Technol.* **2024**, *6*, 62–76. <https://doi.org/10.3390/cleantechnol6010005>

Academic Editor: Rosa Taurino

Received: 11 October 2023

Revised: 22 December 2023

Accepted: 28 December 2023

Published: 3 January 2024



**Copyright:** © 2024 by the authors. Licensee MDPI, Basel, Switzerland. This article is an open access article distributed under the terms and conditions of the Creative Commons Attribution (CC BY) license (<https://creativecommons.org/licenses/by/4.0/>).

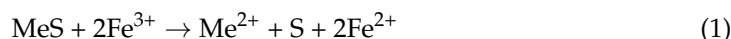
## 1. Introduction

Chemolithotrophic organisms utilize inorganic components for their metabolic functions through oxidation processes, where elements such as sulphur and iron represent essential components to conduct electron transfer processes and amino acid synthesis [1,2]. Chemolithotrophic microorganisms have essential functions in biogeochemical processes occurring in nature. In the processes of assimilation and dissimilatory of sulphur compounds, the assimilatory processes involve the biosynthesis of cellular compounds, and the dissimilatory processes use sulphur compounds as electron acceptors or donors [3]. Some reports indicate the use of inorganic sulphur substrates, such as tetrathionate, for energy production by the oxidation of tetrathionate and the formation of sulfates [4,5] or thiosulfates in microorganisms such as *Thiobacillus acidophilus* [6] as well as other acidophiles [7], where the metabolic mechanisms in the sulfoxidation of tetrathionate are the Sox enzyme complex, and the enzymes sulphur dioxygenase and sulphur oxygenase reductase [8]. The use of thiosulfate for its oxidation to sulfate can be carried out by an enzymatic route, where the Sox enzyme complex converts thiosulfate to sulfate without intermediate compounds, and through the metabolism of chemolithotrophic microorganisms that oxidize thiosulfate to form tetrathionate where thiosulfate is an intermediary oxidation compound

into sulfate [9]. In contrast, the processes involved in energy production are performed at a low pH [10]. The SOX enzyme complex can perform sulfate reduction to H<sub>2</sub>S as a dissimilatory process since the anion is transported from the extracellular environment into the cytoplasm facilitated by sulfate permease, in which two protons are transported for each disulfide anion. In the cytoplasm, the dissimilatory process is ATP-dependent since it is an endergonic mechanism, by the formation of sulphur pyrophosphate and ATP, forming adenosine 5'-phosphosulfate (APS) as an intermediate, catalyzed by the enzyme APS reductase. This metabolism is performed in anaerobic respiration in conjunction with menaquinone enzymes that transfer electrons, forming an electron transport complex [11]. Microorganisms such as *Acidithiobacillus ferrooxidans*, which is chemolithotrophic [12], use ferric ions and sulphur as a source of energy under anaerobic conditions, carrying out the process of cellular respiration through sulphur [13], where the activation of specific genes and quorum sensing produces an increase in its electroactive capacity, which is related to the ability to obtain energy by oxidizing solid ferrous substrates [14].

Microorganisms such as *Desulfovibrio* [15] use anaerobic respiration mechanisms where sulphur acts as a final electron acceptor, and the electron exchange is conducted by the quinol-cytochrome C oxidoreductase enzyme complex present in the cell membrane, where the main product of reduced sulphur is H<sub>2</sub>S due to anaerobic respiration [16].

The chemical reaction (Equation (1)) describing the mechanism in the bioleaching of sulfide ores described by Boon, Heijnen, and Hansford (1998) [17] shows the recovery of lead from galena by the effect of ferrous ions in the 9K culture medium through an indirect mechanism [18]:



In energy generation processes, there are two mechanisms to transfer electrons from the cell to an electron acceptor material or anode, which occur through direct and/or indirect mechanisms. The direct mechanism is one of the most favourable in the transport of electrons because it requires direct physical contact between the cell and the anode, where direct contact can be achieved through nanotubes (pilis), cytochromes, or biofilm, and microorganisms such as *Geobacter* transfer electrons through pilis and cytochromes present in the cell wall [19]. To achieve a more efficient electron transfer, the anode must be composed of a biocompatible material, mainly carbon-based materials, such as graphite [20].

The most commonly used microorganisms in microbial fuel cells are cyanobacteria [21], algae [22], and autotrophic bacteria [23]. Autotrophic bacteria possess metabolic pathways that can support the production of electric current and the fixation of CO<sub>2</sub> [24]. The generation of energy in conventional bioelectrochemical systems from the oxidation of organic compounds through the metabolism of some microorganisms by redox processes, where metal ions have been found to promote this type of process [25].

Inorganic mineral substrates have been used in sedimentary or wetland-type microbial fuel cell systems, such as the study presented by Ge et al. (2020), where the use of pyrite in one of these systems obtained a maximum voltage of 176 mV, since the pyrite participates in the oxidation of N and P compounds, attributed to the cycle Fe<sup>+2</sup> Fe<sup>+3</sup> [26]. Sulphate-reducing microorganisms such as *Desulfovibrio desulphuricans* can transfer electrons through nanotubes or pilis in their cell membrane when the substrate is not in a soluble state since these microorganisms are naturally found in anaerobic sediments [27]. The application of these types of microorganisms using insoluble mineral matrixes as substrates in bioelectrochemical systems has not been thoroughly studied. The effect of inorganic mineral substrates in bioelectrochemical systems indicates that their addition has positive effects on the stability of the voltage produced in such systems applied in wastewater by decreasing the resistance of the aqueous phase at the anode [28]. Previous studies have evaluated the energetic prospective of oxidation processes of sulphide mineral compounds presented by Ni et al. (2016) using acidophilic microorganisms with acid mine wastewater where they obtained a maximum voltage of 107 mV [29].

The objective and main contribution of this exploratory study is to evaluate the prospective voltage produced by a reductive process of a PbS sulphur-containing mineral

matrix by chemoautotrophic microorganisms, for future application in bioelectrochemical systems.

## 2. Materials and Methods

### 2.1. Growing Medium

The selected growing medium was based on the MR medium [30], with some modifications to facilitate the isolation of chemolithotrophic, alkalophilic, halotolerant, and sulfate-oxidizing microorganisms:  $(\text{NH}_4)\text{SO}_4$  1 g/L,  $\text{K}_2\text{HPO}_4$  0.08 g/L,  $\text{CaCl}_2 \cdot 2\text{H}_2\text{O}$  0.375 g/L,  $\text{NaHCO}_3$  2 g/L,  $\text{MgCl}_2$  4.5 g/L,  $\text{NaCl}$  8 g/L,  $\text{MnO}_2$  1.3 g/L, with an initial pH adjustment at 10. It was then autoclaved at 121 °C and 15 psi for 15 min. Agarose at a concentration of 14 g/L was used as the solidifying medium.

### 2.2. Isolation

The microorganisms used in this research were isolated from tailings from the AUT-LAN mining industry. Isolation was performed with an MR growth medium incubated at 30 °C with agitation at 160 rpm. In the first isolation phase, the sterile culture medium was inoculated with 15% (*w/v*) of mine tailings. Cell growth analysis was performed by counting in a Neubauer chamber. Later, serial dilutions were performed for the identification of strains, and as colonies present on plates were identified, reseeded was performed by plate extension for each of the colonies.

### 2.3. Microorganism Identification

After centrifugation at 14,000 rpm, inoculated MR medium was recovered in a 1.5 mL Eppendorf microtube with the necessary growth until a visible pellet of cells was formed at the bottom of the microtube.

Extraction of genomic DNA from the microorganisms present in the bacterial inoculum was made using the Thermo Scientific geneJET genomic DNA purification kit, to later visualize the presence of genomic DNA in a 1% agarose gel (95 V, 55 min).

From the extracted genomic DNA, the 16S ribosomal gene was amplified for identification using universal primers: 27F(5'-AGAGTTTGATCCTGGCTCAG-3') and 1492R(5'-GGTACCTTG TTACGACTT-3') [31]. The amplification of the V3 region of the 16S ribosomal gene was performed using the reaction mixture for PCR of 25 µL DreamTaq Hot Start Green PCR Master Mix (2X) Thermo Scientific (Waltham, MA, USA), 5 µL 27F, 5 µL 1492 R, 10 µL DNA genomic, and 5 µL nuclease-free water. Cycling parameters for PCR were programmed with a preheating at 72 °C for 3 min, followed by 34 cycles at 95 °C for 30 s, 60 °C for 30 s, and 72 °C for 1 min and 30 s. After completion, the amplification was confirmed by electrophoresis (95 V, 55 min) in agarose gel (1.5%). The obtained fragment of interest identified on the agarose gel was removed from the gel with a scalpel, purified and concentrated with a QIAquick kit QIAGEN (Venlo, The Netherlands), and sequenced for further analysis.

### 2.4. Determination of Inorganic Mineral Sulphur Species

To determine and characterize the sulphur mineral species present in the solid fraction, a Rigaku X-ray diffractometer miniflex model was used, with an X-ray tube  $\text{CuK}\alpha$   $\lambda$  1.5418 Å 40 kV and 15 mA. The XRD analysis of the samples was performed from a scan of 5–90° in  $2\theta$ , performing Rietvel refinement with PDLX2 software version 2.8 and semiquantitative analysis according to the Reference Intensity Ratio (RIR) method [32,33] where the intensity for a compound  $\alpha$ , is given by the ratio of the volume fraction of the compound ( $c_\alpha$ ), for the constant  $K_1$ , divided by the linear absorption coefficient of the sample  $\mu_m$  according to Equation (2).

$$I_\alpha = \frac{K_1 C_\alpha}{\mu_m} \quad (2)$$

The quantification of sulphates present in the liquid fraction was determined using the 4500 turbidimetric method for the determination of  $\text{SO}_4^{2-}$  of the standard methods for the examination of water and wastewater [34].

The production of inorganic sulphur compounds in the gaseous fraction quantified as  $\text{H}_2\text{S}_{(g)}$  was determined by direct measurement with BIOGAS5000 equipment.

To identify the role played by PbS in the concentrate within the system, as well as to identify the mechanisms of electrical energy generation, the concentrations of inorganic sulphur species in the gaseous fraction ( $\text{H}_2\text{S}$ ), in the liquid fraction ( $\text{SO}_4$ ), and in the solid fraction were determined.

### 2.5. Salt Bridge

The salt bridge solution [35,36] was made up of a solution of 35 g of KCl, diluted in 100 mL of phosphate buffer (pH 7) and agarose (10%) as a solidifying agent, sterilized in an autoclave (15 min, 105 °C and 1 atm), then carefully poured into glass tubes of 25 mm diameter and 200 mm length in a U shape for solidification.

### 2.6. Cathode

Shown in Figure 1, this consisted of a 500 mL Erlenmeyer flask with 250 mL of PBS (pH 7) used to increase the conductivity of the cathode system. The gaseous fraction of the cathode was at ambient conditions. The material selected as cathode is a graphite cylinder of 2 mm diameter and 100 mm long with a surface area of 634.6 mm<sup>2</sup> (without considering the porosity of the material).

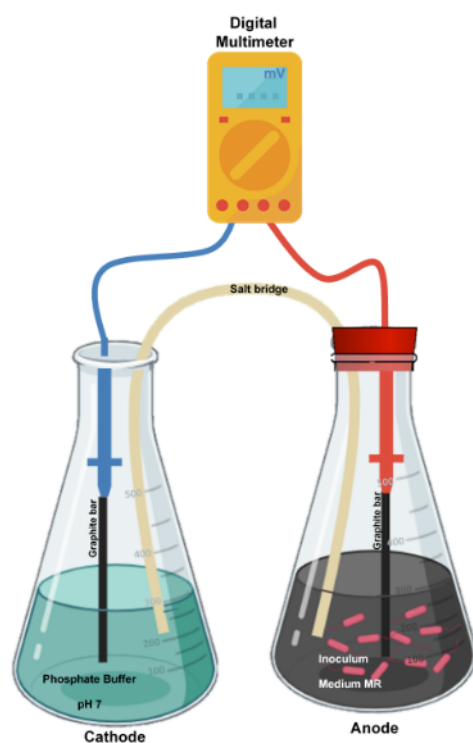


**Figure 1.** System Configuration.

### 2.7. Anode

Shaped as shown in Figure 1, it was developed according to a 2<sup>2</sup> experimental design with replicates. The experimental units contained 15% (*w/v*) of mineral concentrate previously sterilized in dry heat [37]. The material selected as an anode (working electrode) was a graphite cylinder of 2 mm in diameter and 100 mm long with a surface area of 634.6 mm<sup>2</sup> (without considering the porosity of the material) for each of the experimental units.

The experimental test flask acting as an anode was incubated at 30 °C and 160 rpm. The experimental units were purged at each monitoring with a CO<sub>2</sub> flow rate of 2 L/min and were subsequently resealed.

### 2.8. Experimental Design

A 2<sup>2</sup> factorial experimental design (Table 1) was used with substrate [Grow medium MR (MC) and MR + inorganic mineral (C)] and gas fraction [air (atm) and CO<sub>2</sub> (AN)] as categorical factors. Evaluated responses were voltage (mV), redox (mV), pH (-), cell density (cell/mL), H<sub>2</sub>S (ppm), SO<sub>4</sub><sup>-2</sup> (ppm), and PbS (%). Quadratic regressions were performed, and an ANOVA ( $p < 0.05$ ) was used for statistical analysis.

**Table 1.** Factorial experimental design for anode.

Factors	Categorical Levels	
Substrate	Culture medium MR (MC)	MR+ inorganic mineral (C)
Gas fraction	Atmospheric (Atm)	CO <sub>2</sub> (AN)

### 2.9. Voltage Measurements

The measurements were performed by connecting the anode and cathode to a commercial digital multimeter as illustrated in Figure 1, measuring every 24 h.

### 2.10. Anode Cell Density

With the use of scanning electron microscopy analyzed under a low vacuum at 10 KV [38] the cell density of microorganisms adhered to the graphite cylinder (anode) was evaluated as biofilm formation. The cell density was obtained by performing topographical image analysis with software Image J version 1.52p [39,40] identifying cells adhered to the working electrode and adjusting the concentration according to the electrode area with Kurt De Vos's cell counter from the University of Sheffield, Academic Neurology. The cell density of the planktonic cells was determined by counting in a Neubauer chamber.

## 3. Results and Discussion

### 3.1. Isolation and Identification

After the extraction of DNA from the bacterial inoculum, it was visualized in 1% of agarose gel (Figure 2A) and the integrity of the DNA can be observed, as a band marked above 10 Kb of the molecular marker with which the 16S ribosomal gene is amplified for the identification of microorganisms. In Figure 2B, the PCR product showed a 1500 bp fragment in column 1, which corresponds to the expected fragment size [41]. Fragments of 1500 bp were obtained from the PCR product and the sequences obtained were analyzed with BLAST software version 2.15.0 to obtain the percentage of identity of the sequence of interest.

The microorganism identified in the sequence obtained was *Bacillus clausii* with 96% identity for the sequenced fragment. It has been found that some strains of *Bacillus clausii* can grow in anaerobic conditions [42] and have been isolated from various environments, usually found in soils, marine soils [43,44], and biofilms of corroding environments [45]. Although this was the only identified microorganism, the consortium was made up of various types of microorganisms, determining that a highly reducing environment requires protection for the consortium. This protection can occur in the formation of the biofilm that hosts *Bacillus clausii*, and other species.

### 3.2. Characterization of Inorganic Mineral Substrate

The mineral concentrate was characterized by X-ray diffraction (XRD), where the mineralogical composition was obtained according to the diffraction pattern and mineral composition (Table 2).

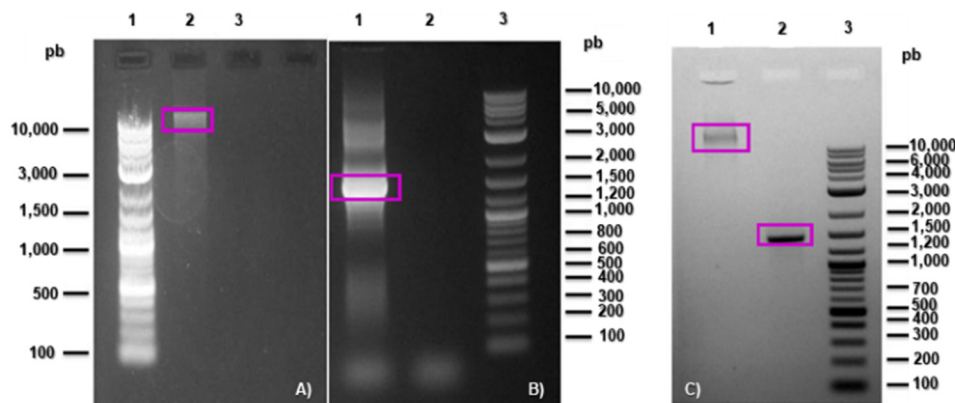


**Figure 2.** (A) Agarose gel 1%, 1 DNA ladder 10 Kb, 2 Genomic DNA, (B) agarose gel 1%, 1 product of PCR 1500 pb, 3 DNA ladder 10 Kb, (C) agarose gel 1%, 1 Genomic DNA, 2 product of PCR 1500 pb purified, 3 DNA ladder 10 Kb.

**Table 2.** Mineralogic composition.

Compound	Formula	Concentration (%)
Galena	PbS	77
Sulphur species of lead	PbS	14.5
Sulphur	S	5
Others	--	19.5

The mineral concentrate contains 84.4% of lead sulfide (PbS) as galena corresponding to the diffraction pattern where the main peaks showed angles of 30.11°, 26°, 43.1° in 2θ (Figure 3) for cubic galena COD 9013403 and 15% of tetragonal chalcopyrite COD 9015636.

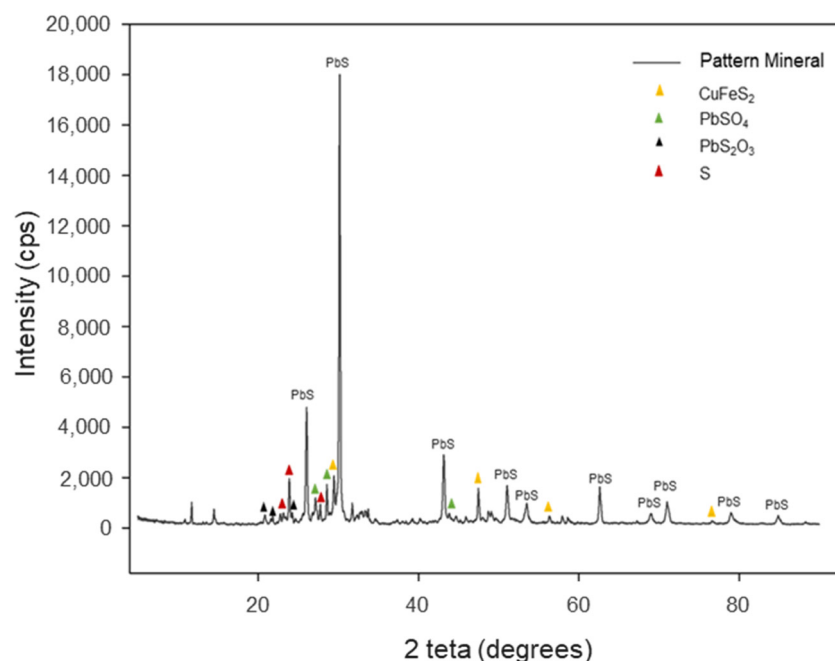


**Figure 3.** X-ray diffraction pattern for mineral concentrate.

### 3.3. Cell Growth

To evaluate the microbiological growth in each of the anodic experimental units, planktonic cell density measurements were made in the culture medium (Figure 4) by Neubauer chamber counting and in the anodic material (graphite rod) by SEM for sessile cells.

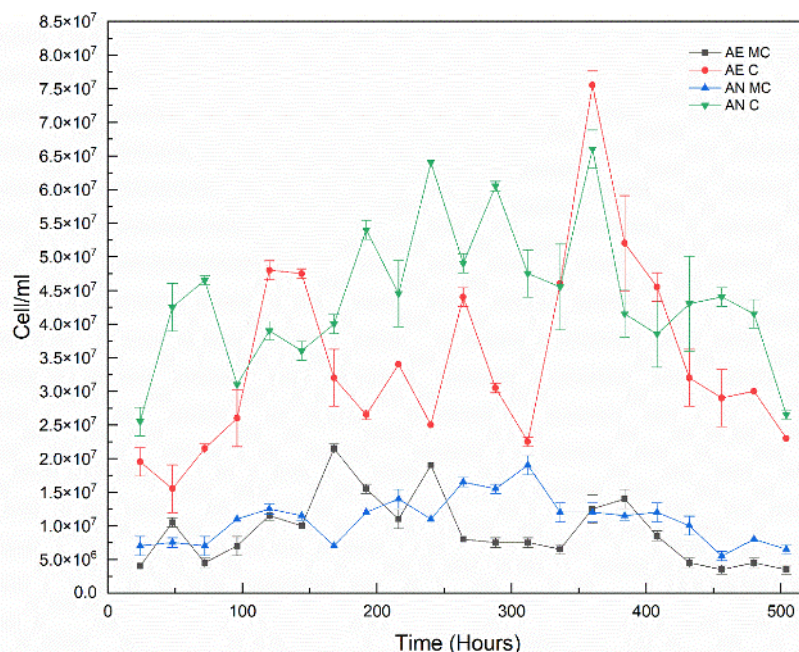


**Figure 4.** Planktonic cell density under experimental design conditions (AE: atmospheric conditions, AN: CO<sub>2</sub> purged, C: mineral concentrate, MC: culture medium).

The analysis showed that the highest planktonic cell density was found in the treatments added with the mineral substrate, both in the culture medium and in the graphite bars. An ANOVA ( $p < 0.05$ ) was performed to evaluate the effect of substrate and gas fraction on cell density, where the substrate was identified as the only factor with a significant effect on cell density, in the quantification in liquid medium, as well as in the graphite rod. Also, the addition of the mineral concentrate had a positive effect ( $p < 0.05$ ) on the increase of planktonic cell density compared to using the MR culture medium without concentrate. This behaviour in the cell growth of the bacterial inoculum is attributed to the natural characteristics of the microorganisms, since they are native to soils, they possess characteristics to carry out their metabolic processes from inorganic mineral sources, where minerals, offering surface and support, provide nutrients and favour the production of biofilms, where component transfer interfaces are generated between the solid substrates and the cells [46]. Microorganisms of the species Gammaproteobacteria have been reported to grow using iron-containing solid substrates promoting the oxidation of ferrous ions using a direct mechanism [47], since the solid minerals play a role as terminal electron acceptors and donors in cellular respiration [46,48], which is linked to the increase in cell density in the presence of inorganic mineral substrates. However, to attribute the increase in cell density to the mineral substrate used, it is important to identify the role that it is playing in the microbiological system.

### 3.4. Use of Inorganic Sulphur as a Substrate

For the obtained diffraction pattern, PbS was identified as the major component in mineral species such as galena with 77% abundance (Table 2). Other sulphur species identified were CuFeS<sub>2</sub> (chalcopyrite), PbSO<sub>4</sub>, FeSO<sub>4</sub>, Pb(S<sub>2</sub>O<sub>3</sub>), and S (Figure 3).

In the experimental units added with mineral concentrate, the solid fractions were analyzed by XRD, where the mobility of sulphur species is shown in Figure 5 for days 2, 10, 14, and 18 (D-2, D-10, D-14, and D-18) under aerobic and anaerobic conditions (purged with CO<sub>2</sub>). The days selected for the evaluation of the solid fractions correspond to the microbial growth stages identified in Figure 4. For the experiments with added mineral, it was possible to identify that there was mobility for galena according to the XRD pattern (Figure 3) and the determined intensity of the peak pattern, which according to Cullity and

Stock (2014) [49] is proportional to the volume fraction of the compound in the samples for the RIR method.

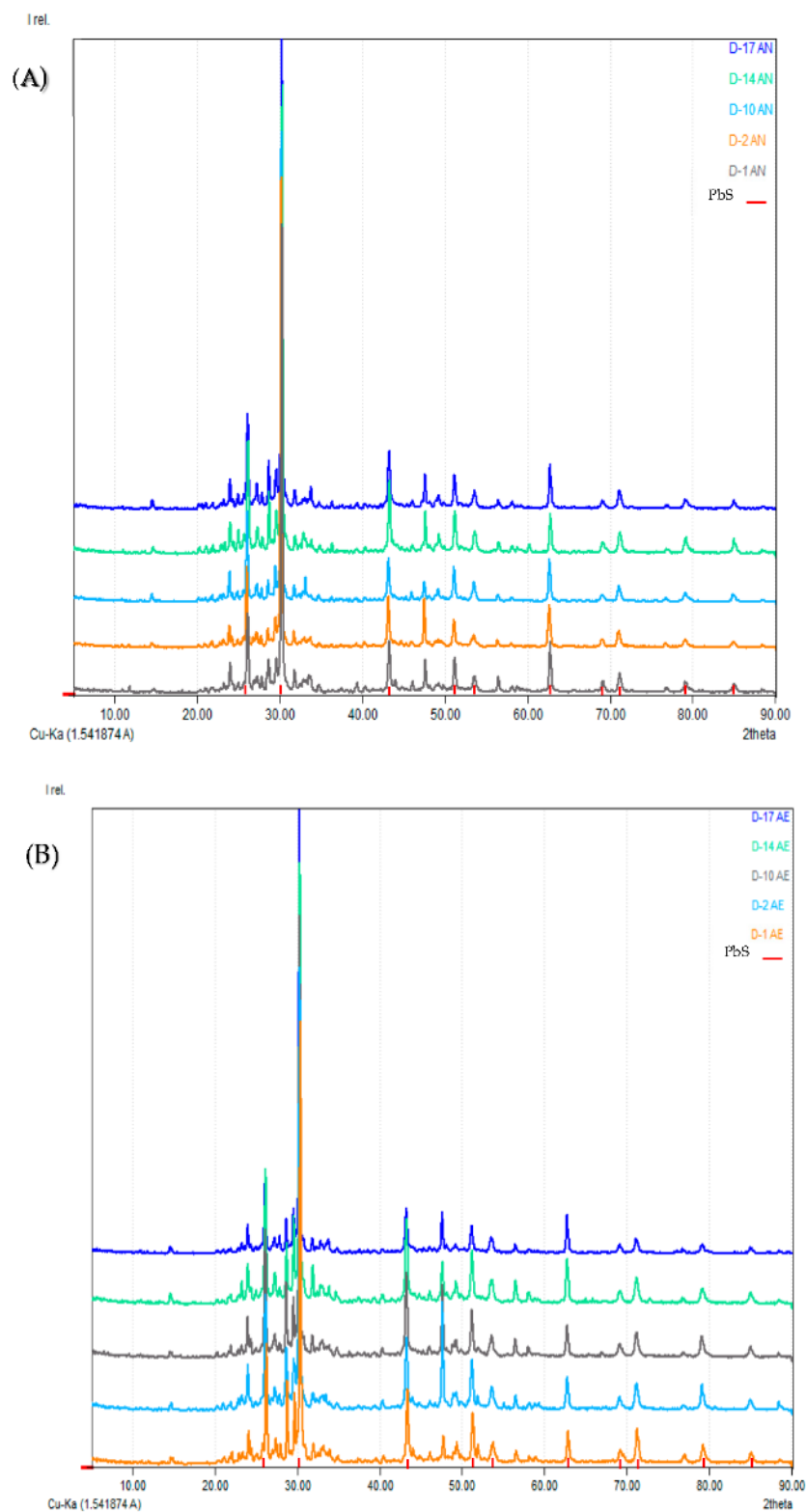


**Figure 5.** Diffraction patterns for days 2, 10, 14, and 17; (A) Aerobic conditions (B) anaerobic condition (CO<sub>2</sub> purged).

The variation in the intensity of the peak pattern identified for galena is attributed to the change in concentration of the species as shown in Figure 5A,B, where the diffraction

pattern was identified under anaerobic conditions corresponding to PbS with greater intensity at time 10. This possibly occurred due to the decrease in the concentration of components such as sulphur, where it was possible to identify the reduction in the intensity of the peak pattern corresponding to the sulphur of D-17 concerning the diffraction pattern of D-2. For aerobic conditions, the intensity of the peak pattern decreased for compounds such as  $\text{PbSO}_4$  and S, at all times. However, the diffraction pattern identified for PbS suffered an increase for D-10, which could be attributed to the use of other compounds present in the mineral, which increases the proportion of PbS in the solid sample, which could be evaluated according to the concentration (%) of the components present in the sample (Figure 6).

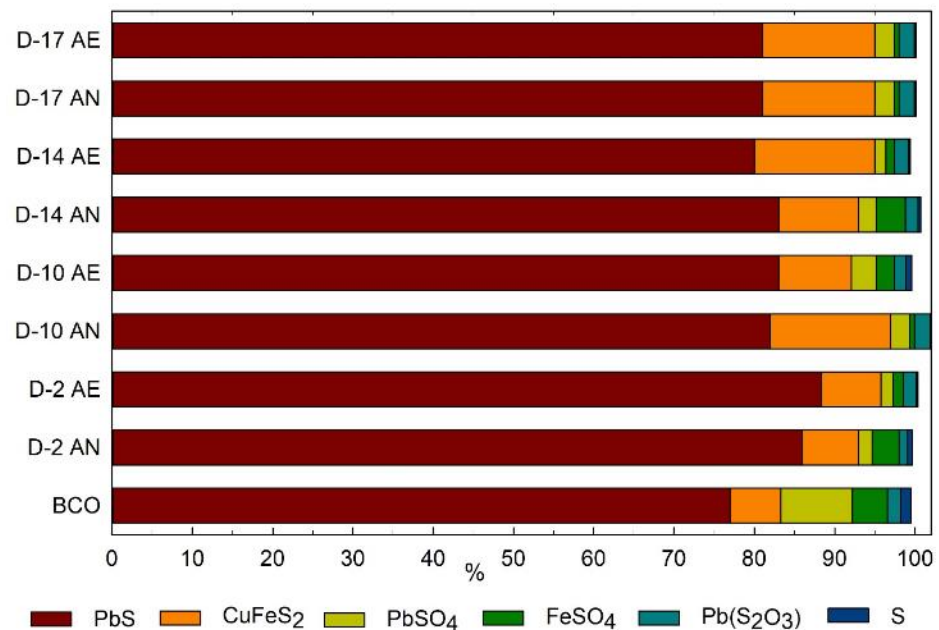


**Figure 6.** Mineralogical analysis using DRX of the experimental units for days 2, 10, 14, and 18 (D-2, D-10, D-14, D-18) in conditions AE: atmospheric conditions and AN:  $\text{CO}_2$ .

In addition, it was identified that the reduction of PbS concentration (Table 3) in the solid fraction is associated with the bioconversion of the mineral into other sulfide species, such as lead sulphates in the solid fraction, which increases the proportion present in the solid fraction, as well as the presence of soluble sulphates in the culture medium, which could be attributable to passive mechanisms [50]. Zhao et al. (2019) studied this mechanism and found mesophilic chemolithotrophic microorganisms used in biohydrometallurgy for the bioleaching of refractory sulphide compounds [50]. The highest  $\text{H}_2\text{S}$  production was 1150 ppm (Table 3) in the gaseous fraction under anaerobic conditions and with mineral substrate. This is strong evidence suggesting that sulphur bioconversion reactions by microbiological activity are occurring. Some of the main compounds that promote redox reactions are sulphur compounds, such as PbS, which undergoes a decrease of 4.3% in weight for aerobic conditions, and 7% under anaerobic conditions. Such redox reactions occurred after the oxidation led to form sulphated compounds and, subsequently, the sulphur of these compounds became elemental sulphur and  $\text{H}_2\text{S}$ , where it was identified that the production of H ions generates the acidification of the culture medium under anaerobic conditions with added PbS, in which greater acidification of the medium was achieved under aerobic conditions. For the experimental units containing only culture medium as substrate, it was identified that there was no variation in pH for aerobic conditions. However, under anaerobic conditions, there was a slight acidification of the medium, which probably was promoted by the addition of  $\text{CO}_2$ , which in contact with the culture medium can form carbonic acid ( $\text{H}_2\text{CO}_3$ ) [51]. In processes of reduction of sulphur compounds by the action of microorganisms, it has been reported that  $\text{H}_2\text{S}$  is

produced under anaerobic conditions, due to the reduction of oxidized sources of sulphur; this process is related to the mechanism of anaerobic respiration in which H<sub>2</sub>S is produced by the reduction of sulphates and thiosulphates in anaerobic respiration, since these act as final electron acceptors [52]. Unlike sulphur-oxidizing microorganisms, which at pH of 9.5 and salinity of 20 g/L are reported to promote the conversion of sulphur compounds to sulphate by bio-oxidation, using nitrate as the final electron acceptor [53].

**Table 3.** Inorganic sulphur compounds.

Condition	Substrate	H <sub>2</sub> S (ppm)	SO <sub>4</sub> <sup>-2</sup> (ppm)	PbS (%)		Voltage (mV)
				Ti	TF	
AE	C	479	32.22 ± 1.71	86	81	586 ± 26.1
AE	MC	35.15	10.90 ± 0.28	*	*	438 ± 29.6
AN	MC	171.5	10.00 ± 1.57	*	*	383.5 ± 57.2
AN	C	1150.0	1344.44 ± 116.27	88	80	647 ± 17.6

\* No PbS was added to these experimental units.

### 3.5. Voltage Production

Output voltage in the experimental units (Figure 7) was monitored starting at 96 h, where the exponential growth stage begins for the conspecific, and up to 500 h, where the death phase is identified or where cell density decreases. At 96 h of growth, all experimental units start at a voltage of 400 mV.

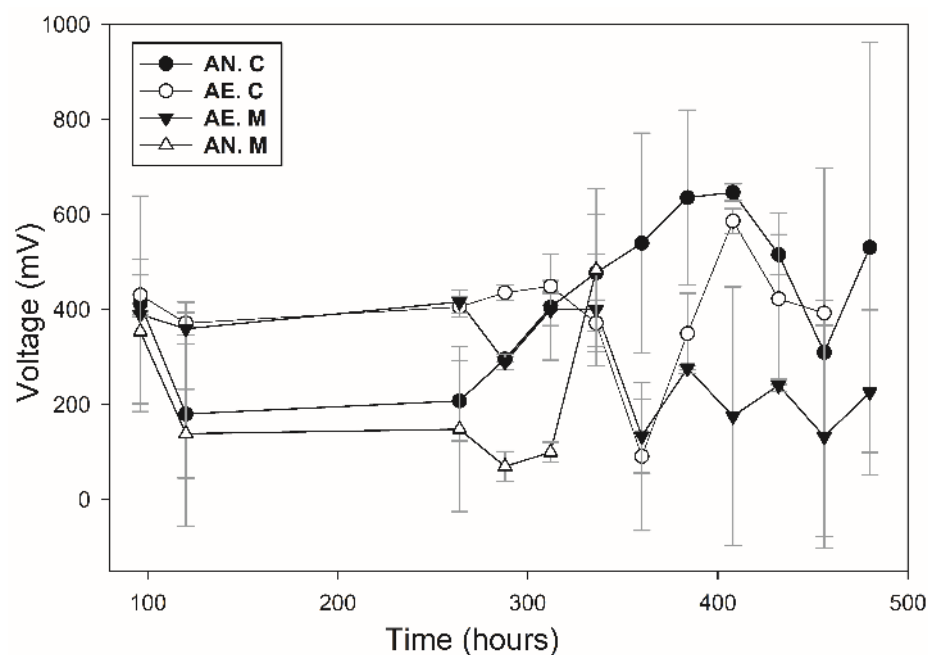


**Figure 7.** Voltage production monitoring in the experimental units (AE: atmospheric conditions, AN: CO<sub>2</sub> purged, C: mineral concentrate PbS, M culture medium).

The controls without inoculum shown in Table 4 maintained constant voltages during the 500 h monitoring, where the minimum voltage obtained was 27 mV for the experimental unit with mineral and under anaerobic conditions. The experimental units without mineral and under aerobic and anaerobic conditions maintained a voltage production of 40 mV. The voltage produced by the controls was generated by the interaction between the salts in the culture medium and the added mineral, with the salts and mineral compounds acting as electrolytes.

**Table 4.** Production of voltage, H<sub>2</sub>S, and sulfates in controls without inoculum.

Condition	Substrate	H <sub>2</sub> S (ppm)	SO <sub>4</sub> <sup>-2</sup> (ppm)	Voltage (mV)
AE	C	0	20	48.1
AE	MC	0	10	42.3
AN	MC	0	10	40.2
AN	C	0	260	27

C: PbS added in these experimental units, MC: Culture medium, AE: aerobic conditions. AN: anaerobic conditions.

In the experimental units, different conditions were tested for voltage production with the consortium, it was found that the voltage production was higher than that obtained in the controls, where the obtained voltage of 400 mV demonstrates that the consortium is composed of electroactive microorganisms, which interact with the substrate to produce electrical energy. It was also found that under anaerobic and aerobic conditions with added mineral produced a voltage of 644.68 mV and 574 mV, respectively, at a time of 400 h. These values were higher than those found in the units without solid substrate, which produced a maximum voltage of 474 mV and 403 mV for anaerobic and aerobic conditions, respectively.

The obtained results were higher compared to the results obtained by González-Paz et al. (2022) [54], who used iron-reducing bacteria with a mineral medium, obtaining the highest voltage (0.3 V) using a salt bridge. Huang et al. (2023) [55] evaluated the use of a consortium of filamentous sulphate-reducing microorganisms from sediments, applied in a sediment fuel cell with an inorganic substrate source, obtaining a maximum voltage of 100 mV. However, compared to studies where sulphate-reducing microorganisms are used, the voltage obtained is slightly lower, but within the range (Table 5), in the different applications of bioelectrochemical systems we can identify that the voltage produced is competitive with systems that apply conductive polymers and organic substrates which are presented in Table 4 of the review of Kuznetsova et al. (2023) [56].

The increase in voltage production associated with the solid sulphite substrate source is related to higher cell density in the growth kinetics. This is attributed to the interaction between microorganisms and solid substrates, involving the use of cytochromes that act as promoters of oxidation-reduction reactions in direct and indirect mechanisms since the metabolites produced by the microorganisms and the mechanisms used in bioleaching are the same involved in the transfer of extracellular electrons in electroactive microorganisms [57,58].

The concentration of sessile cells attached by the biofilm onto the graphite electrode is one of the main promoters of voltage production in the system. Evaluating the cell density of these cells (Figure 8) allowed us to identify that the conditions of high concentration of sessile cells on the electrode were the ones that produced the highest voltages in the systems containing solid substrates with inoculated minerals. The increase in voltage production provides positive information regarding the electroactivity of the cells that compose the inoculum since these cells carry out redox reactions while interacting with the substrate, due to oxidation processes executed in the first stages of the formation of sulphates, to later perform reduction processes of oxidized sulphur compounds until reaching the production of H<sub>2</sub>S.

The mechanisms employed by the consortium agree with the reported processes in the literature (Table 5), indicating that obtaining a higher voltage in the units with a higher presence of biofilm, shows that the electron transport is carried out by direct mechanisms from the cells to the graphite electrode, possibly by the interaction of the proteins present in the cell membrane, which since they tested positive in the oxidase test, it indicates that these microorganisms have cytochromes type C, which can be detectable by this biochemical test [59].

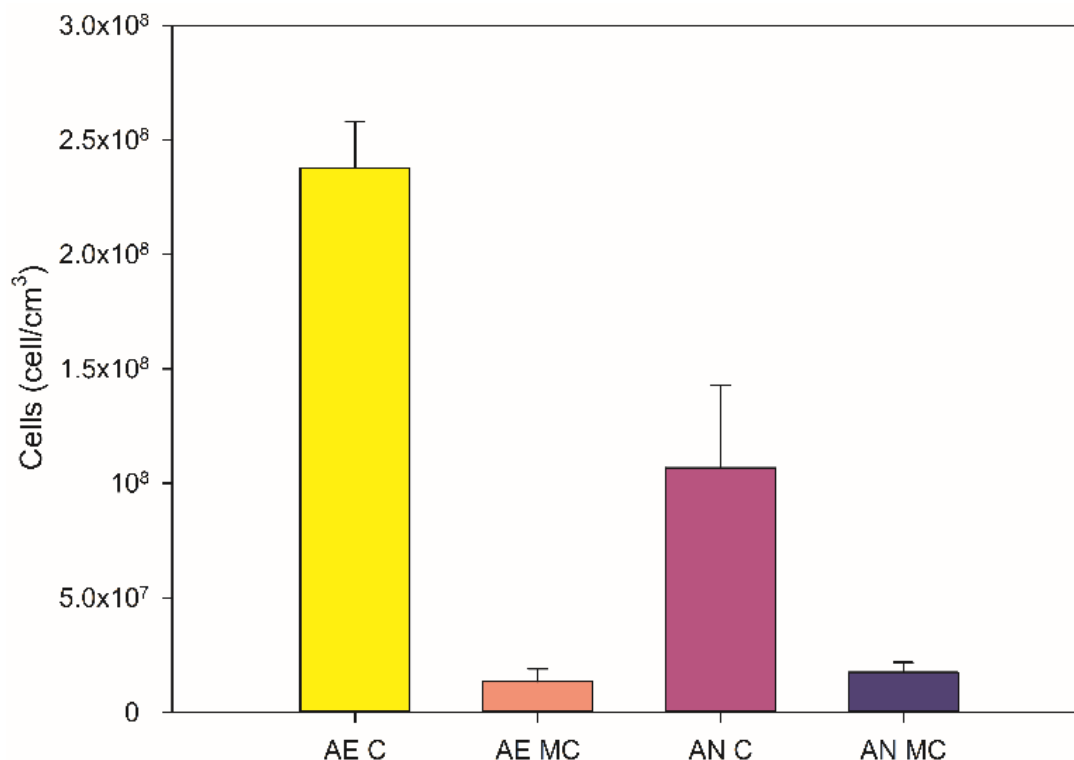


**Figure 8.** Sessile cell density under experimental design conditions at 400 h in graphite bar (AE: atmospheric conditions, AN: CO<sub>2</sub> purged, C: mineral concentrate, MC: culture medium).

**Table 5.** Comparison of energy production.

System Description	Substrate	Voltage Produced (mV)	Inoculum	References
Batch	PbS	664		Present Work
Batch + salt bridge	Acetate + Fe <sup>+3</sup>	220–380	Iron-reducing consortium	González-Paz et al. (2022) [52]
Two chambered laboratory scale microbial fuel cell	Zeolite + MgSO <sub>4</sub>	750	Natural sulphate-reducing bacterium consortium	Angelov et al. (2013) [60]
Cylindrical SMFCs	Sulphate-rich sediments	30–40	<i>L. varians</i> GY32	Huang et al. (2023) [53]

#### 4. Conclusions

The microorganisms that compose the bacterial inoculum possess electroactive properties by using as substrate an inorganic source of mineral sulphur composed of PbS as the major compound. The microorganisms conduct the oxidation of sulphur, which is reduced to the formation of H<sub>2</sub>S. The use of sulphur as the last electron acceptor in the process promotes the production of up to 644 mV in anoxic conditions at 400 h, and the energy production is attributed to the adhesion of bacteria on the graphite electrode, where the transfer of electrons is carried out directly between the biofilm formed by the bacteria to the electrode. The evaluated microorganisms showed a promising perspective for application in bioelectrochemical systems using inorganic substrates, which have not been thoroughly studied in the development of technologies for bioenergy production.

**Author Contributions:** Conceptualization, H.M.R.; data curation, S.C.G.G.; funding acquisition, E.D.; investigation, S.C.G.G. and J.A.R.-C.; methodology, S.C.G.G. and J.A.R.-C.; project administration, D.R.J.; supervision, J.A.R.-C. and D.R.J.; visualization, H.M.R.; writing—original draft, S.C.G.G.; writing—review and editing, D.E.Z.-Á., P.G.V.O., and D.R.J. All authors have read and agreed to the published version of the manuscript.

**Funding:** This research received no external funding.

**Institutional Review Board Statement:** Not applicable.

**Informed Consent Statement:** Not applicable.

**Data Availability Statement:** Data are contained within the article.

**Conflicts of Interest:** The authors declare no conflict of interest.

## References

1. Matin, A. Organic nutrition of chemolithotrophic bacteria. *Annu. Rev. Microbiol.* **1978**, *32*, 433–468. [[CrossRef](#)] [[PubMed](#)]
2. Kumar, R.; Pundir, S. Bacterial Cell, Classification and Required Essential Contents for Growth. *Asian J. Pharm. Technol.* **2021**, *11*, 181–187. [[CrossRef](#)]
3. Dahl, C. A biochemical view on the biological sulphur cycle. In *Environmental Technologies to Treat Sulphur Pollution: Principles and Engineering*, 2nd ed.; Lens, P.N.L., Ed.; IWA Publishing: London, UK, 2020.
4. Sulonen, M.L.K.; Lakaniemi, A.M.; Kokko, M.E.; Puhakka, J.A. The effect of anode potential on bioelectrochemical and electrochemical tetrathionate degradation. *Bioresour. Technol.* **2017**, *226*, 173–180. [[CrossRef](#)] [[PubMed](#)]
5. Sulonen, M.L.K.; Lakaniemi, A.M.; Kokko, M.E.; Puhakka, J.A. Long-term stability of bioelectricity generation coupled with tetrathionate disproportionation. *Bioresour. Technol.* **2016**, *216*, 876–882. [[CrossRef](#)] [[PubMed](#)]
6. Meulenberg, R.; Scheer, E.J.; Pronk, J.T.; Hazeu, W.; Bos, P.; Kuenen, J.G. Metabolism of tetrathionate in *Thiobacillus acidophilus*. *FEMS Microbiol. Lett.* **1993**, *112*, 167–172. [[CrossRef](#)]
7. Sulonen, M.L.K.; Kokko, M.E.; Lakaniemi, A.M.; Puhakka, J.A. Electricity generation from tetrathionate in microbial fuel cells by acidophiles. *J. Hazard. Mater.* **2014**, *284*, 182–189. [[CrossRef](#)] [[PubMed](#)]
8. Wang, R.; Lin, J.Q.; Liu, X.M.; Pang, X.; Zhang, C.J.; Yang, C.L.; Gao, X.-Y.; Lin, C.-M.; Li, Y.-Q.; Li, Y.; et al. Sulphur oxidation in the acidophilic autotrophic *Acidithiobacillus* spp. *Front. Microbiol.* **2019**, *10*, 3290.
9. Alam, M.; Fernandes, S.; Mandal, S.; Rameez, M.J.; Bhattacharya, S.; Peketi, A.; Mazumdar, A.; Ghosh, W. <sup>34</sup>S enrichment as a signature of thiosulfate oxidation in the ‘Proteobacteria’. *FEMS Microbiol. Lett.* **2021**, *368*, fnab073. [[CrossRef](#)]
10. Doyle, L.E.; Marsili, E. Weak electricigens: A new avenue for bioelectrochemical research. *Bioresour. Technol.* **2018**, *258*, 354–364. [[CrossRef](#)]
11. Wing, B.A.; Halevy, I. Intracellular metabolite levels shape sulphur isotope fractionation during microbial sulfate respiration. *Proc. Natl. Acad. Sci. USA* **2014**, *111*, 18116–18125. [[CrossRef](#)]
12. Chabert, N.; Bonnefoy, V.; Achouak, W. Quorum sensing improves current output with *Acidithiobacillus ferrooxidans*. *Microb. Biotechnol.* **2018**, *11*, 136–140. [[CrossRef](#)]
13. Ohmura, N.; Sasaki, K.; Matsumoto, N.; Saiki, H. Anaerobic Respiration Using Fe<sup>3+</sup>, S<sup>0</sup>, and H<sub>2</sub> in the Chemolithoautotrophic Bacterium *Acidithiobacillus ferrooxidans*. *J. Bacteriol.* **2002**, *184*, 2081–2087. [[CrossRef](#)] [[PubMed](#)]
14. González, A.; Bellenberg, S.; Mamani, S.; Ruiz, L.; Echeverría, A.; Soulère, L.; Doutheau, A.; Demergasso, C.; Sand, W.; Queneau, Y.; et al. AHL signalling molecules with a large acyl chain enhance biofilm formation on sulphur and metal sulfides by the bioleaching bacterium *Acidithiobacillus ferrooxidans*. *Appl. Microbiol. Biotechnol.* **2013**, *97*, 3729–3737. [[CrossRef](#)] [[PubMed](#)]
15. Keller, K.L.; Wall, J.D. Genetics and molecular biology of the electron flow for sulfate respiration in *Desulfovibrio*. *Front. Microbiol.* **2011**, *2*, 135. [[CrossRef](#)] [[PubMed](#)]
16. Koch, T.; Dahl, C. A novel bacterial sulphur oxidation pathway provides a new link between the cycles of organic and inorganic sulphur compounds. *ISME J.* **2018**, *12*, 2479–2491. [[CrossRef](#)] [[PubMed](#)]
17. Boon, M.; Snijder, M.; Hansford, G.S.; Heijnen, J.J. The oxidation kinetics of zinc sulphide with *Thiobacillus ferrooxidans*. *Hydrometallurgy* **1998**, *48*, 171–186. [[CrossRef](#)]
18. Baba, A.A.; Adekola, F.A.; Atata, R.F.; Ahmed, R.N.; Panda, S. Bioleaching of Zn(II) and Pb(II) from Nigerian sphalerite and galena ores by mixed culture of acidophilic bacteria. *Trans. Nonferrous Met. Soc. China (Engl. Ed.)* **2011**, *21*, 2535–2541. [[CrossRef](#)]
19. Saratale, G.D.; Saratale, R.G.; Shahid, M.K.; Zhen, G.; Kumar, G.; Shin, H.-S.; Choi, Y.-G.; Kim, S.-H. A comprehensive overview on electro-active biofilms, role of exo-electrogens and their microbial niches in microbial fuel cells (MFCs). *Chemosphere* **2017**, *178*, 534–547. [[CrossRef](#)]
20. Selim, H.M.M.; Kamal, A.M.; Ali, D.M.M.; Hassan, R.Y.A. Bioelectrochemical Systems for Measuring Microbial Cellular Functions. *Electroanalysis* **2017**, *29*, 1498–1505. [[CrossRef](#)]
21. Visser, P.M.; Verspagen, J.M.; Sandrini, G.; Stal, L.J.; Matthijs, H.C.; Davis, T.W.; Paerl, H.W.; Huisman, J. How rising CO<sub>2</sub> and global warming may stimulate harmful cyanobacterial blooms. *Harmful Algae* **2016**, *54*, 145–159. [[CrossRef](#)]

22. Ramaraj, R.; Tsai, D.D.W.; Chen, P.H. Carbon dioxide fixation of freshwater microalgae growth on natural water medium. *Ecol. Eng.* **2015**, *75*, 86–92. [[CrossRef](#)]
23. Singh, S.K.; Rahman, A.; Dixit, K.; Nath, A.; Sundaram, S. Evaluation of promising algal strains for sustainable exploitation coupled with CO<sub>2</sub> fixation. *Environ. Technol.* **2016**, *37*, 613–622. [[CrossRef](#)] [[PubMed](#)]
24. Rossi, F.; Olguin, E.J.; Diels, L.; De Philippis, R. Microbial fixation of CO<sub>2</sub> in water bodies and in drylands to combat climate change, soil loss and desertification. *New Biotechnol.* **2015**, *32*, 109–120. [[CrossRef](#)] [[PubMed](#)]
25. Lovley, D.R. The microbe electric: Conversion of organic matter to electricity. *Curr. Opin. Biotechnol.* **2008**, *19*, 564–571. [[CrossRef](#)] [[PubMed](#)]
26. Ge, X.; Cao, X.; Song, X.; Wang, Y.; Si, Z.; Zhao, Y.; Wang, W.; Tesfahunegn, A.A. Bioenergy generation and simultaneous nitrate and phosphorus removal in a pyrite-based constructed wetland-microbial fuel cell. *Bioresour. Technol.* **2020**, *296*, 122350. [[CrossRef](#)]
27. Eaktasang, N.; Kang, C.S.; Lim, H.; Kwean, O.S.; Cho, S.; Kim, Y.; Kim, H.S. Production of electrically-conductive nanoscale filaments by sulfate-reducing bacteria in the microbial fuel cell. *Bioresour. Technol.* **2016**, *210*, 61–67. [[CrossRef](#)] [[PubMed](#)]
28. Du, Y.; Feng, Y.; Teng, Q.; Li, H. Effect of inorganic salt in the culture on microbial fuel cells performance. *Int. J. Electrochem. Sci.* **2015**, *10*, 1316–1325. [[CrossRef](#)]
29. Ni, G.; Christel, S.; Roman, P.; Wong, Z.L.; Bijmans, M.F.M.; Dopson, M. Electricity generation from an inorganic sulphur compound containing mining wastewater by acidophilic microorganisms. *Res. Microbiol.* **2016**, *167*, 568–575. [[CrossRef](#)]
30. AGreene, C.; Patel, B.K.C.; Sheehy, A.J. *Deferribacter thermophilus* gen. nov., a Novel Thermophilic Manganese and Iron Reducing Bacterium Isolated from a Petroleum Reservoir. *Strain* **1997**, *47*, 505–509.
31. Nandhana, G.; Rajasulochana, P. Genome Sequence Analysis of the Bacillus Cereus Isolated From Soil Sample. *Ann. Rom. Soc. Cell Biol.* **2021**, *25*, 2625–2636.
32. Hubbard, C.R.; Snyder, R.L. RIR—Measurement and Use in Quantitative XRD. *Powder Diffr.* **1988**, *3*, 74–77. [[CrossRef](#)]
33. Mirahati, R.Z.; Amalia, Y.; Juliyanto, M.; Larasati, L.; Putri, A. Mineral Preparation Using Rod Mill for Mineral Galena Characterization Silika Galena Pirit. *RSF Conf. Ser. Eng. Technol.* **2021**, *1*, 355–362.
34. Rice, E.W.; Bridgewater, L.; American Public Health Association (Eds.) *Standard Methods for the Examination of Water and Wastewater*; American Public Health Association: Washington, DC, USA, 2012; Volume 10, p. 541.
35. Deval, A.; Dikshit, A.K. Construction, Working and Standardization of Microbial Fuel Cell. *APCBEE Procedia* **2013**, *5*, 59–63. [[CrossRef](#)]
36. Min, B.; Cheng, S.; Logan, B.E. Electricity generation using membrane and salt bridge microbial fuel cells. *Water Res.* **2005**, *39*, 1675–1686. [[CrossRef](#)]
37. Trevors, J.T. Sterilization and inhibition of microbial activity in soil. *J. Microbiol. Methods* **1996**, *26*, 53–59. [[CrossRef](#)]
38. Liberman, L.; Kleinerman, O.; Davidovich, I.; Talmon, Y. Micrograph contrast in low-voltage SEM and cryo-SEM. *Ultramicroscopy* **2020**, *218*, 113085. [[CrossRef](#)] [[PubMed](#)]
39. Rueden, C.T.; Schindelin, J.; Hiner, M.C.; DeZonia, B.E.; Walter, A.E.; Arena, E.T.; Eliceiri, K.W. ImageJ2: ImageJ for the next generation of scientific image data. *BMC Bioinform.* **2017**, *18*, 529. [[CrossRef](#)]
40. Nichele, L.; Persichetti, V.; Lucidi, M.; Cincotti, G. Quantitative evaluation of ImageJ thresholding algorithms for microbial cell counting. *OSA Contin.* **2020**, *3*, 1417. [[CrossRef](#)]
41. Zeng, L.; Huang, J.; Zhang, Y.; Qiu, G.; Tong, J.; Chen, D.; Zhou, J.; Luo, X. An effective method of DNA extraction for bioleaching bacteria from acid mine drainage. *Appl. Microbiol. Biotechnol.* **2008**, *79*, 881–888. [[CrossRef](#)]
42. Obata, F.; Murota, H.; Shibata, S.; Ozuru, R.; Fujii, J. Investigation of Bacteria from Spoiled Bottled Salad Dressing Leading to Gas Explosion. *Yonago Acta Med.* **2022**, *65*, 207–214. [[CrossRef](#)]
43. Kumar, C.G.; Joo, H.S.; Koo, Y.M.; Paik, S.R.; Chang, C.S. Thermostable alkaline protease from a novel marine haloalkalophilic *Bacillus clausii* isolate. *World J. Microbiol. Biotechnol.* **2004**, *20*, 351–357. [[CrossRef](#)]
44. Ghosh, A.; Bhardwaj, M.; Satyanarayana, T.; Khurana, M.; Mayilraj, S.; Jain, R.K. *Bacillus lehensis* sp. nov., an alkalitolerant bacterium isolated from soil. *Int. J. Syst. Evol. Microbiol.* **2007**, *57*, 238–242. [[CrossRef](#)] [[PubMed](#)]
45. Aslan, C.; Aulia, N.I.; Devianto, H.; Harimawan, A. Influence of axenic culture of *Bacillus clausii* and mixed culture on biofilm formation, carbon steel corrosion, and methyl ester degradation in B30 storage tank system. *J. Environ. Chem. Eng.* **2022**, *10*, 108013. [[CrossRef](#)]
46. Ng, D.H.P.; Kumar, A.; Cao, B. Microorganisms meet solid minerals: Interactions and biotechnological applications. *Appl. Microbiol. Biotechnol.* **2016**, *100*, 6935–6946. [[CrossRef](#)] [[PubMed](#)]
47. Ye, J.; Joseph, S.D.; Ji, M.; Nielsen, S.; Mitchell, D.R.G.; Donne, S.; Horvat, J.; Wang, J.; Munroe, P.; Thomas, T. Chemolithotrophic processes in the bacterial communities on the surface of mineral-enriched biochars. *ISME J.* **2017**, *11*, 1087–1101. [[CrossRef](#)]
48. Gupta, D.; Guzman, M.S.; Bose, A. Extracellular electron uptake by autotrophic microbes: Physiological, ecological, and evolutionary implications. *J. Ind. Microbiol. Biotechnol.* **2020**, *47*, 863–876. [[CrossRef](#)]
49. Cullity, B.D.; Stock, S.R. *Elements of X-ray Diffraction*, 3rd ed.; Pearson Prentice Hall: Old Bridge, NJ, USA, 2014; Volume 1.
50. Zhao, H.; Zhang, Y.; Zhang, X.; Qian, L.; Sun, M.; Yang, Y.; Zhang, Y.; Wang, J.; Kim, H.; Qiu, G. The dissolution and passivation mechanism of chalcopyrite in bioleaching: An overview. *Miner. Eng.* **2019**, *136*, 140–154. [[CrossRef](#)]
51. Zhong, H.; Fujii, K.; Nakano, Y.; Jin, F. Effect of CO<sub>2</sub> bubbling into aqueous solutions used for electrochemical reduction of CO<sub>2</sub> for energy conversion and storage. *J. Phys. Chem. C* **2015**, *119*, 55–61. [[CrossRef](#)]

52. Arndt, C.; Gaill, F.; Felbeck, H. Anaerobic sulphur metabolism in thiotrophic symbioses. *J. Exp. Biol.* **2001**, *204*, 741–750. [[CrossRef](#)]
53. Singh, R.; Chaudhary, S.; Yadav, S.; Patil, S.A. Bioelectrocatalytic sulfide oxidation by a haloalkaliphilic electroactive microbial community dominated by *Desulfobulbaceae*. *Electrochim. Acta* **2022**, *423*, 140576. [[CrossRef](#)]
54. González-Paz, J.R.; Becerril-Varela, K.; Guerrero-Barajas, C. Iron reducing sludge as a source of electroactive bacteria: Assessing iron reduction in biofilm bacteria, planktonic cells and isolates from a microbial fuel cell. *Arch. Microbiol.* **2022**, *204*, 632. [[CrossRef](#)] [[PubMed](#)]
55. Huang, H.; Yang, Y.; Yang, S.; Yang, X.; Huang, Y.; Dong, M.; Zhou, S.; Xu, M. Filamentous electroactive microorganisms promote mass transfer and sulfate reduction in sediment microbial electrochemical systems. *Chem. Eng. J.* **2023**, *466*, 143214. [[CrossRef](#)]
56. Kuznetsova, L.S.; Arlyapov, V.A.; Plekhanova, Y.A.; Tarasov, S.E.; Kharkova, A.S.; Saverina, E.A.; Reshetilov, A.N. Conductive Polymers and Their Nanocomposites: Application Features in Biosensors and Biofuel Cells. *Polymers* **2023**, *15*, 3783. [[CrossRef](#)] [[PubMed](#)]
57. Yuan, Y.; Zhou, S.; Xu, N.; Zhuang, L. Electrochemical characterization of anodic biofilms enriched with glucose and acetate in single-chamber microbial fuel cells. *Colloids Surf. B Biointerfaces* **2011**, *82*, 641–646. [[CrossRef](#)]
58. Su, W.; Zhang, L.; Tao, Y.; Zhan, G.; Li, D.; Li, D. Sulfate reduction with electrons directly derived from electrodes in bioelectrochemical systems. *Electrochem. Commun.* **2012**, *22*, 37–40. [[CrossRef](#)]
59. Shields, P.; Cathcart, L. Oxidase Test Protocol—Library. *Am. Soc. Microbiol. ASM MicrobeLibrary* **2013**, 1–5. Available online: <http://www.microbelibrary.org/library/laboratory-test/3229-oxidase-test-protocol>. (accessed on 21 December 2023).
60. Angelov, A.; Bratkova, S.; Loukanov, A. Microbial fuel cell based on electroactive sulfate-reducing biofilm. *Energy Convers. Manag.* **2013**, *67*, 283–286. [[CrossRef](#)]

**Disclaimer/Publisher’s Note:** The statements, opinions and data contained in all publications are solely those of the individual author(s) and contributor(s) and not of MDPI and/or the editor(s). MDPI and/or the editor(s) disclaim responsibility for any injury to people or property resulting from any ideas, methods, instructions or products referred to in the content.